Exploring the phase diagram of QCD with two massless quarks with an effective theory

Edgar López Contreras
José Antonio García Hernández
Wolfgang Bietenholz

ICN-UNAM

Table of contents

QCD phase diagram

- Low baryon density: crossover
- $T_c \approx 155$ MeV at $\mu_B = 0$
- Sign problem at $\mu_B \neq 0$
- Hypothetical Critical End Point (CEP)

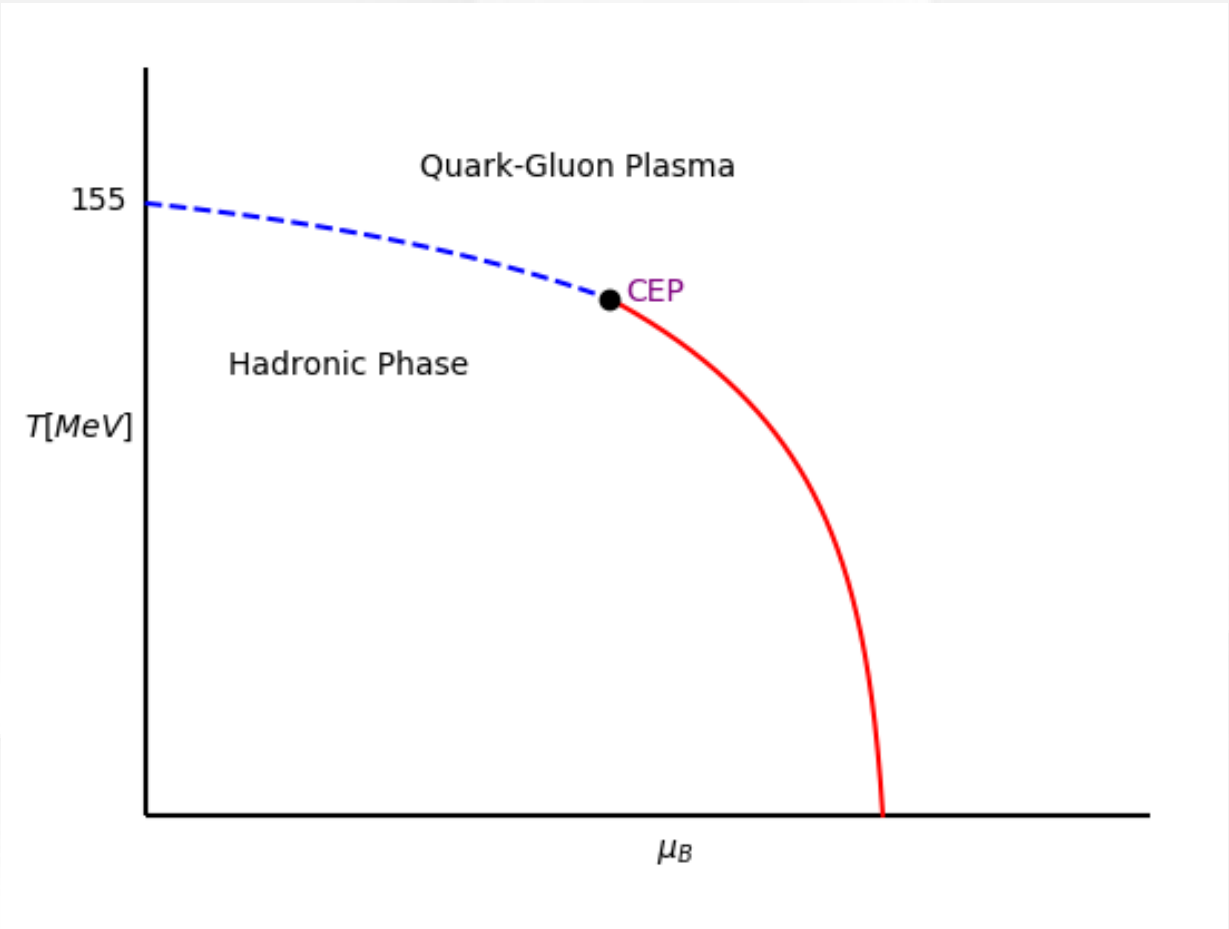

Two flavor QCD in the chiral limit

- $m_{\mathrm{u}}, m_{\mathrm{d}} \ll \Lambda_{\mathrm{QCD}} \approx 300$ MeV
- Global symmetry at $m_{\mathrm{u}} = m_{\mathrm{d}} = 0$:

$$\mathrm{U}(2)_{\mathrm{L}} \otimes \mathrm{U}(2)_{\mathrm{R}} = \mathrm{SU}(2)_{\mathrm{L}} \otimes \mathrm{SU}(2)_{\mathrm{R}} \otimes \mathrm{U}(1)_{\mathrm{V}} \otimes \mathrm{U}(1)_{\mathrm{A}}$$

- Lagrangian:

$$\mathcal{L} = \sum_{f=\mathrm{u},\mathrm{d}} (\bar{q}_{\mathrm{L},f} i \not{D} q_{\mathrm{L},f} + \bar{q}_{\mathrm{R},f} i \not{D} q_{\mathrm{R},f}) - \frac{1}{4} G^a_{\mu\nu} G_a^{\mu\nu}$$

- Chiral Symmetry Breaking (CSB):

$$\mathrm{SU}(2)_{\mathrm{L}} \otimes \mathrm{SU}(2)_{\mathrm{R}} \longrightarrow \mathrm{SU}(2)_{\mathrm{L=R}}$$

- Nambu-Goldstone bosons: π^0, π^+ and π^-.
- Low baryon density: second order phase transition.

3d O(4) non-linear σ model

- Effective theory of QCD,

$$S[\vec{\sigma}] = \frac{1}{2} F_\pi^2 \int d^4x \, \partial_\mu \vec{\sigma}(x) \cdot \partial_\mu \vec{\sigma}(x), \quad \vec{\sigma}(x) \in \mathrm{O}(4)/\mathrm{O}(3) \simeq \mathrm{S}^3,$$

  where $F_\pi \approx 92$ MeV.
- $\pi/2$ Wick rotation of time axis,

$$t_\mathrm{E} = it = 1/T = \beta$$

- High temperature dimensional reduction.
- Euclidean action,

$$S_\mathrm{E}[\vec{\sigma}] = \frac{1}{2} \beta F_\pi^2 \int d^3x \, \partial_i \vec{\sigma}(x) \cdot \partial_i \vec{\sigma}(x), \quad \vec{\sigma}(x) \in \mathrm{O}(4)/\mathrm{O}(3) \simeq \mathrm{S}^3$$

- Spontaneous symmetry breaking locally isomorphic to the CSB,

$$\mathrm{O}(4) \simeq \mathrm{SU}(2)_\mathrm{L} \otimes \mathrm{SU}(2)_\mathrm{R} \longrightarrow \mathrm{O}(3) \simeq \mathrm{SU}(2)_{\mathrm{L}=\mathrm{R}}$$

- Same universality class as the CSB (Skyrme 1961, 1962; Wilczek 1992).

Topological charge $Q[\vec{\sigma}]$

- Topological sectors in 3d.
- Topological charge identify the 3rd homotopy group classes,

$$\pi_3(\mathrm{O}(4)/\mathrm{O}(3) \simeq \mathrm{S}^3) = \mathbb{Z}$$

- Winding number around S^3.
- Conserved under infinitesimal transformations.
- Represents the baryon number (Witten 1983; Adkins et. al 1983). The $\vec{\sigma}(x)$ fields are mesonic but the topological excitations are baryonic.
- Chemical potential μ_B without sign problem.

Lattice regularization

- Lattice regularization,

$$S_{\mathrm{E}}[\vec{\sigma}] = -\beta_{\mathrm{lat}} \left(\sum_{\langle xy \rangle} \vec{\sigma}_x \cdot \vec{\sigma}_y + \mu_{B,\mathrm{lat}} Q[\vec{\sigma}] \right),$$

  sum over nearest neighbors. Lattice units ($a = 1$) and $\beta_{\mathrm{lat}} = \beta F_\pi^2$, $\mu_{B,\mathrm{lat}} = \mu_B / F_\pi^2$.
- Physical units are assigned using the critical temperature at $\mu_B = 0$, $\beta_{c,\mathrm{lat}} = 0.93590$ (Oevers 1996) and $T_c \approx 155$ MeV (Borsanyi et al. 2010),

$$\beta = \frac{\beta_c}{\beta_{c,\mathrm{lat}}} \beta_{\mathrm{lat}} \approx 0.00689\ \mathrm{MeV}^{-1} \beta_{\mathrm{lat}} \qquad \mu_B = \frac{\beta_{c,\mathrm{lat}}}{\beta_c} \mu_{B,\mathrm{lat}} \approx 145\ \mathrm{MeV}\, \mu_{B,\mathrm{lat}}$$

- L^3 lattice volume.
- $\vec{\sigma}(x)$ with periodic boundary conditions. $\vec{\sigma}(x)$ covers all S^3, thus $Q[\vec{\sigma}(x)]$ is integer.

Topological charge on the lattice

- Triangulation of unit lattice cubes in six tetrahedra.
- Spins generate spherical tetraherda.
- Topological charge is the sum of the oriented volumes of the spherical tetrahedra. Murakami's spherical tetrahedron volume formulas (Murakami, 2012).
- Winding number around S^3 is the number of times a reference point is in the spherical tetrahedra.

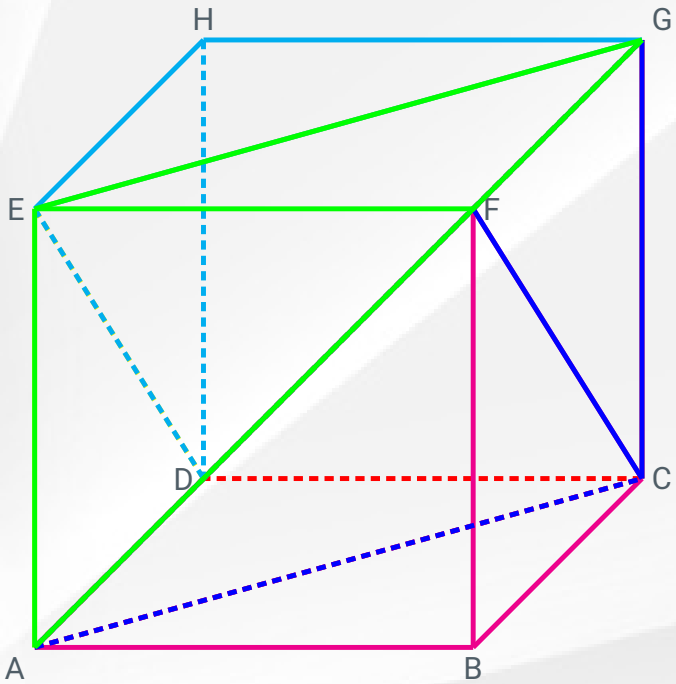

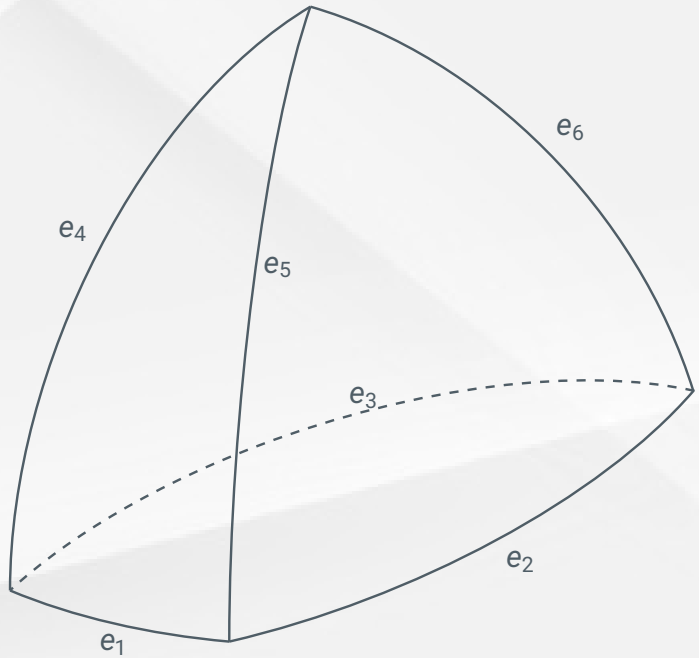

Left: Triangulation of the unit cubes. **Right**: Example of a spherical tetrahedron.

Observables

Magnetization density:

$$m(\beta_{\mathrm{lat}}) = \frac{1}{L^3}\langle|\vec{M}[\vec{\sigma}]|\rangle$$

Energy density:

$$\epsilon(\beta_{\mathrm{lat}}) = \frac{1}{L^3}\langle H[\vec{\sigma}]\rangle$$

Topological charge density:

$$q(\beta_{\mathrm{lat}}) = \frac{1}{L^3}\langle Q[\vec{\sigma}]\rangle$$

Magnetic susceptibility:

$$\chi_M(\beta_{\mathrm{lat}}) = \frac{\beta_{\mathrm{lat}}}{L^3}\left(\langle|\vec{M}[\vec{\sigma}]|^2\rangle - \langle|\vec{M}[\vec{\sigma}]|\rangle^2\right)$$

Specific heat:

$$c_V(\beta_{\mathrm{lat}}) = \frac{\beta_{\mathrm{lat}}^2}{L^3}\left(\langle(H[\vec{\sigma}])^2\rangle - \langle H[\vec{\sigma}]\rangle^2\right)$$

Topological susceptibility:

$$\chi_Q(\beta_{\mathrm{lat}}) = \frac{1}{L^3}\left(\langle(Q[\vec{\sigma}])^2\rangle - \langle Q[\vec{\sigma}]\rangle^2\right)$$

Simulations

- Multicluster algorithm. Collective spin updates.
- Diminish the auto-correlation time of the observables τ, especially of the topological charge.
- T near T_c.
- Baryon chemical potentials,

$\mu_{B,\mathrm{lat}}$	0	0.1	0.2	0.3	0.4	0.5	0.6	0.7	0.8
	0.9	1	1.1	1.2	1.3	1.4	1.5	2.0	2.5
$\mu_B[\mathrm{MeV}]$	0	14.5	29	43.5	58	72.5	87	101.5	116.1
	130.6	145.1	159.6	174.1	188.6	203.1	217.6	290.1	362.7

- L^3 volume lattices.
- Statistics 10^4 field configurations.
- Measurements such that $\tau \approx 1/2$, which is the perfect measurement separation.

Magnetization density

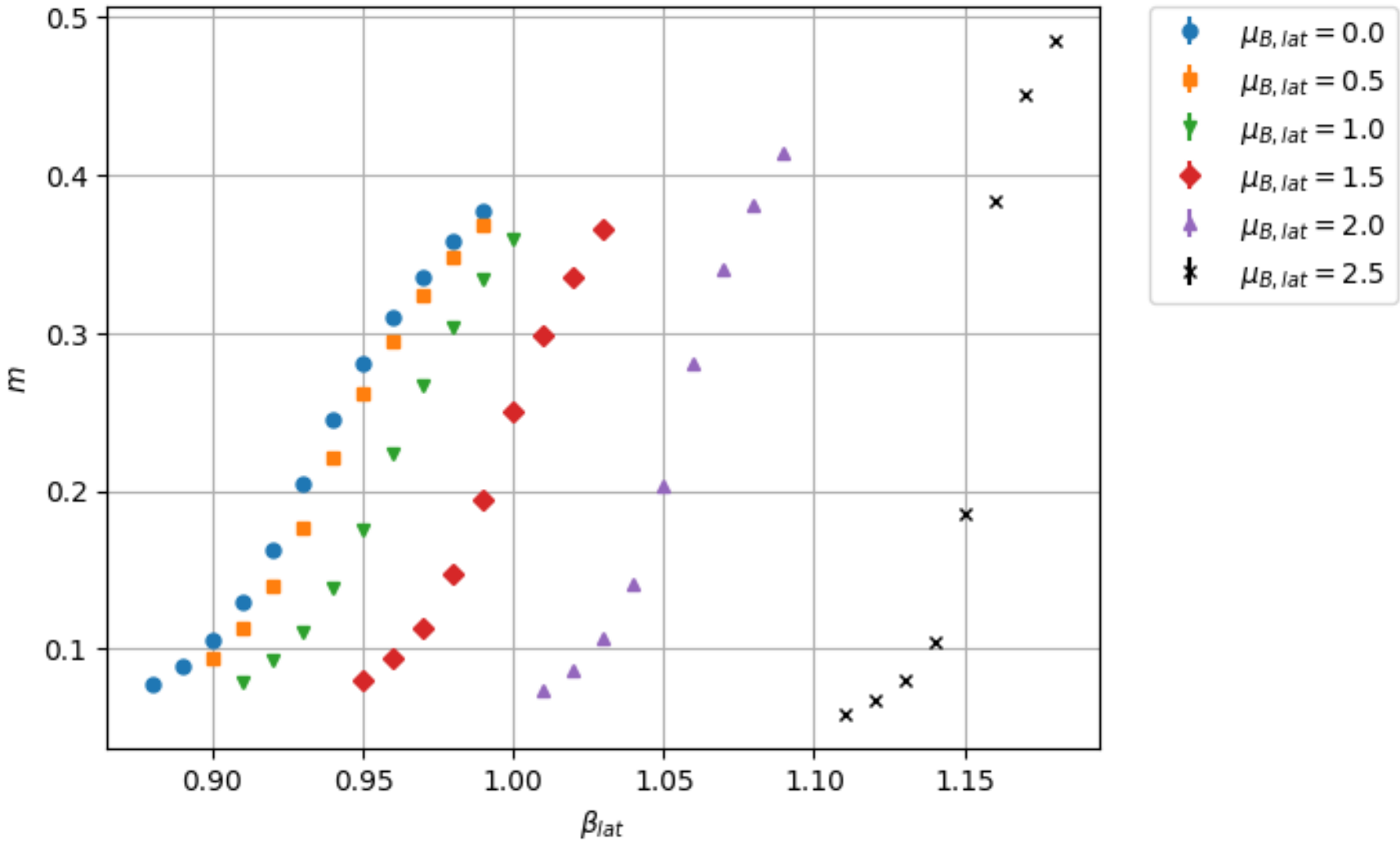

Magnetization density in a lattice of volume 20^3.

Energy density

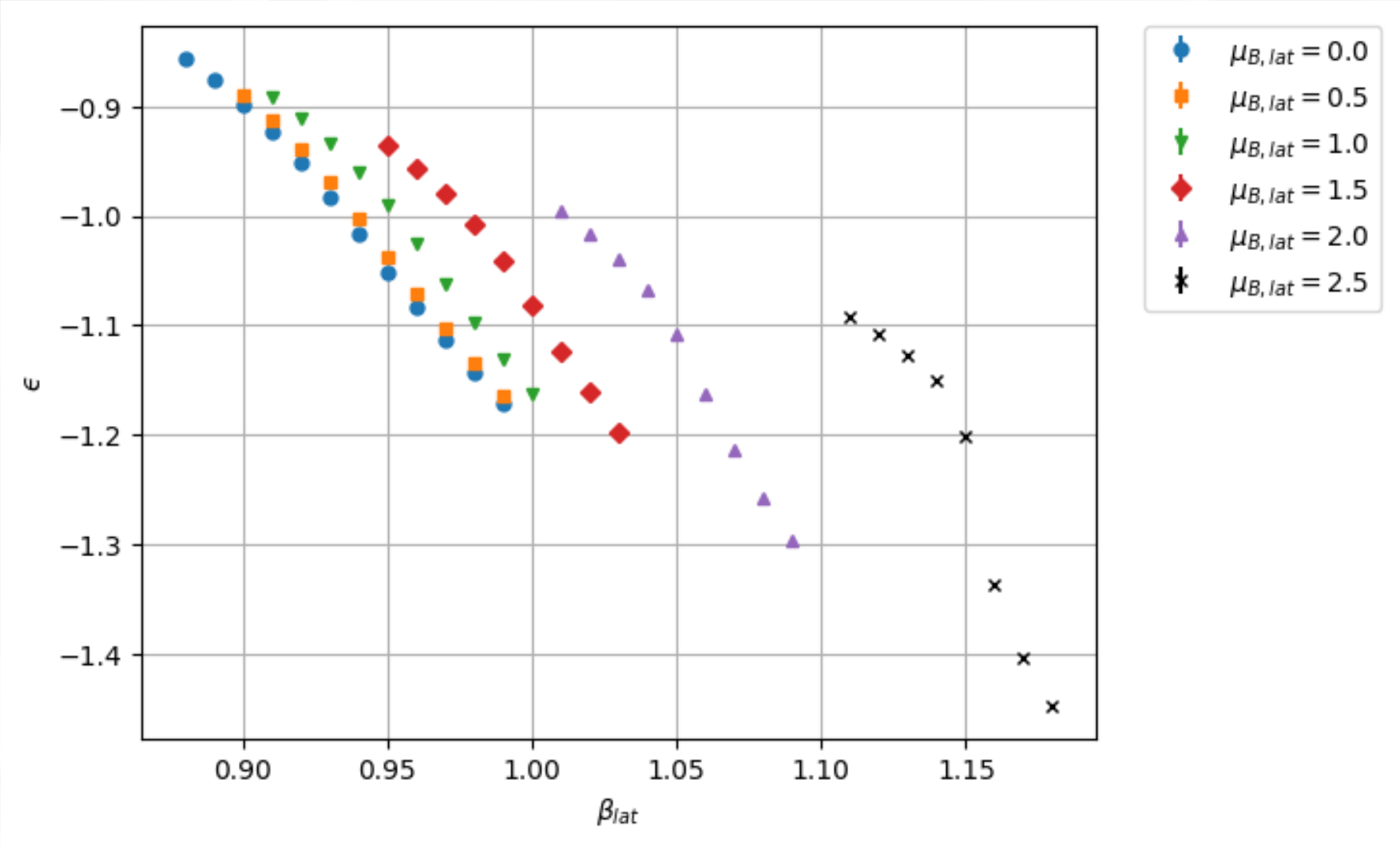

Energy density in a lattice of volume 20^3.

Topological charge density

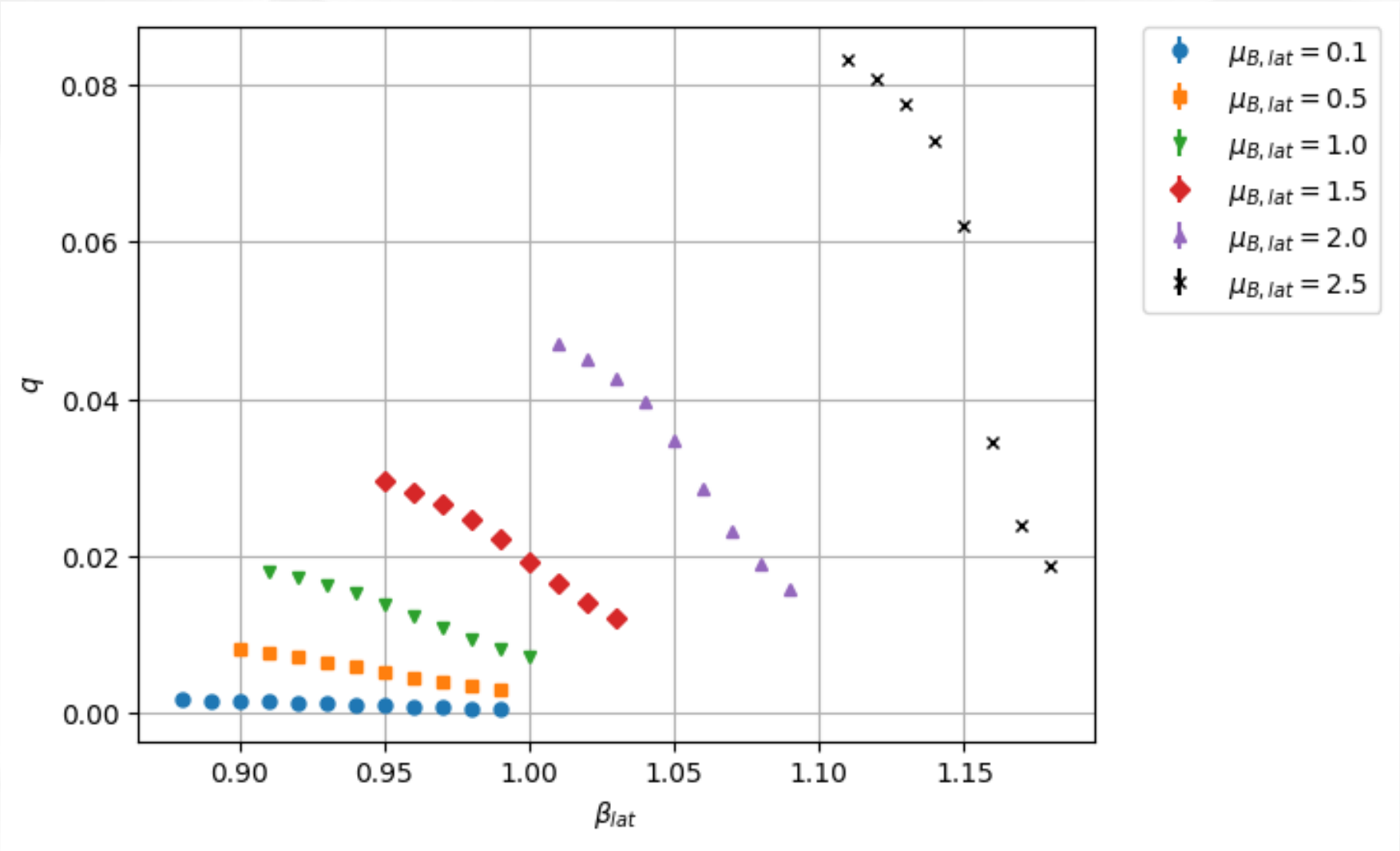

Topological charge density in a lattice of volume 20^3.

Magnetic suscpetibility

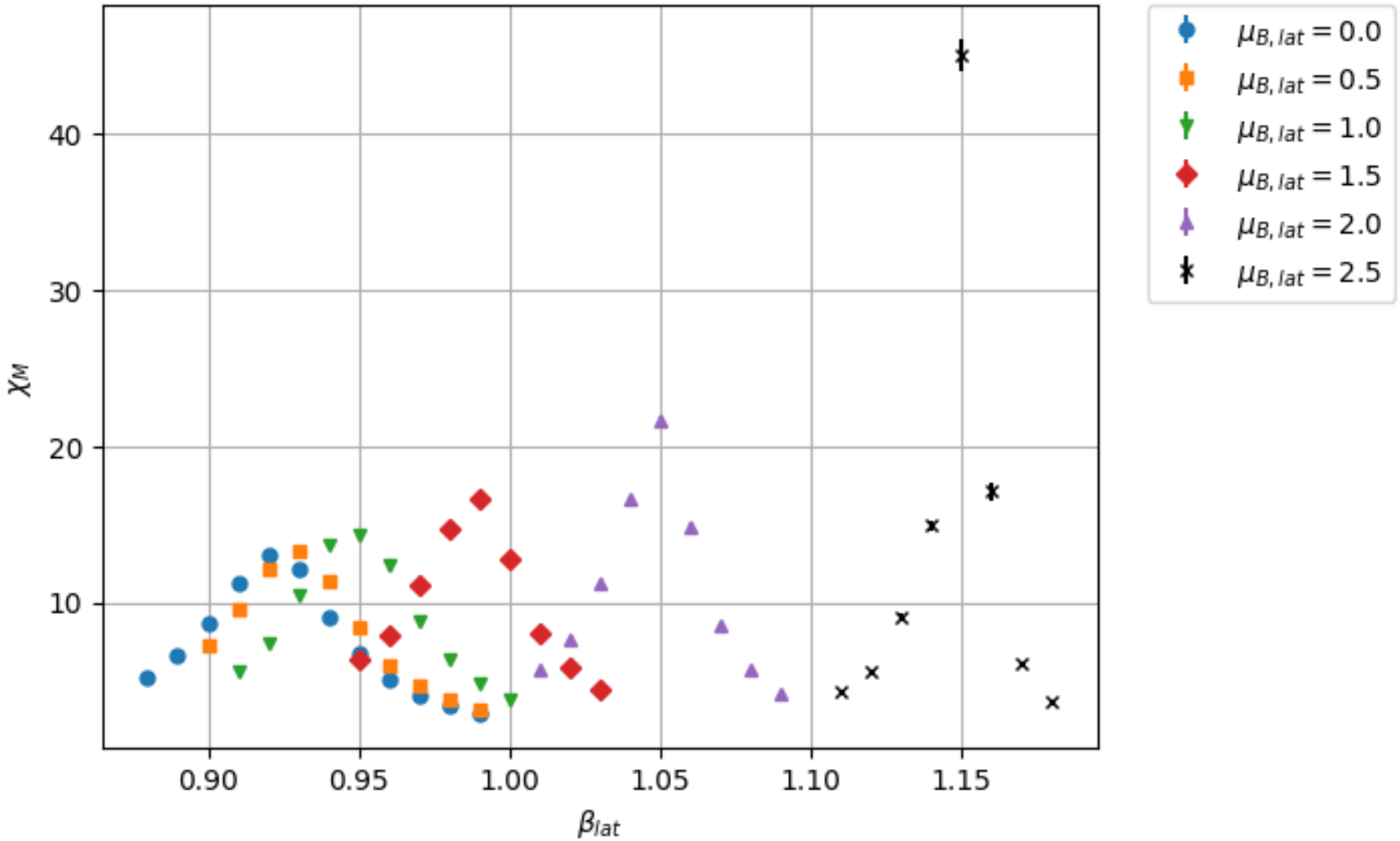

Magnetic susceptibility in a lattice of volume 20^3.

Magnetic susceptibility

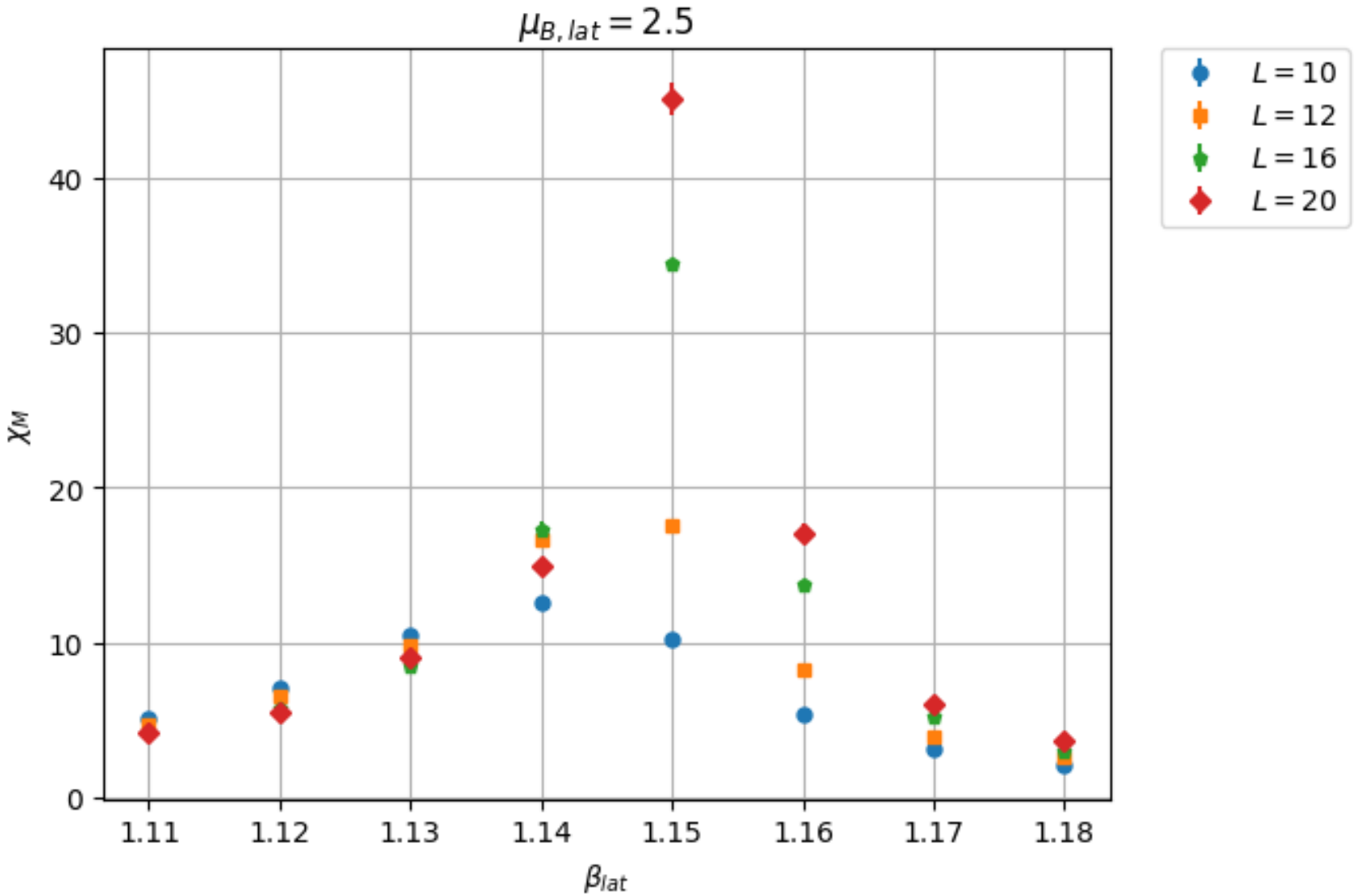

Magnetic susceptibility at $\mu_{B,\mathrm{lat}} = 2.5$ in lattices of volume L^3.

Specific heat

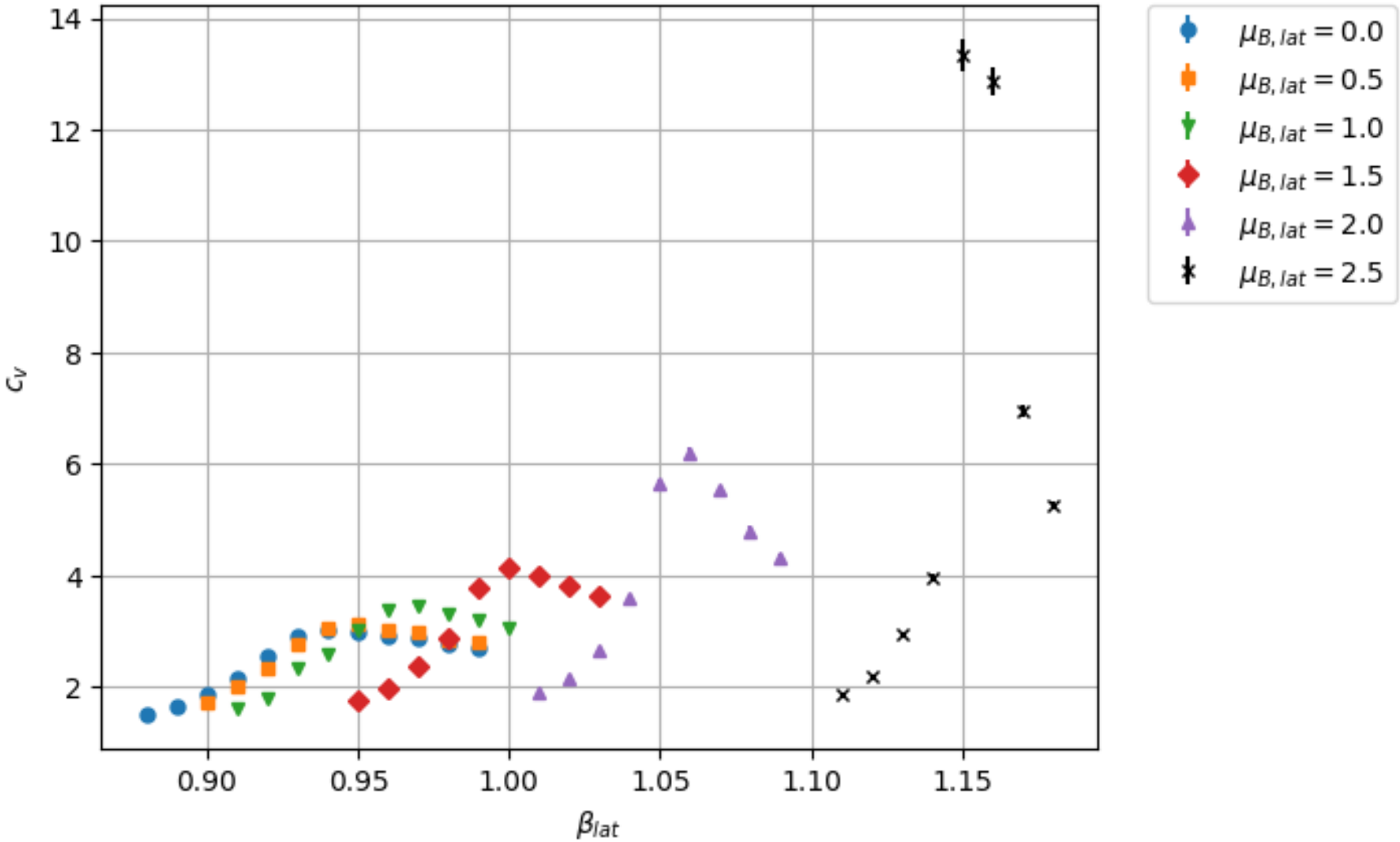

Specific heat in a lattice of volume 20^3.

Specific heat

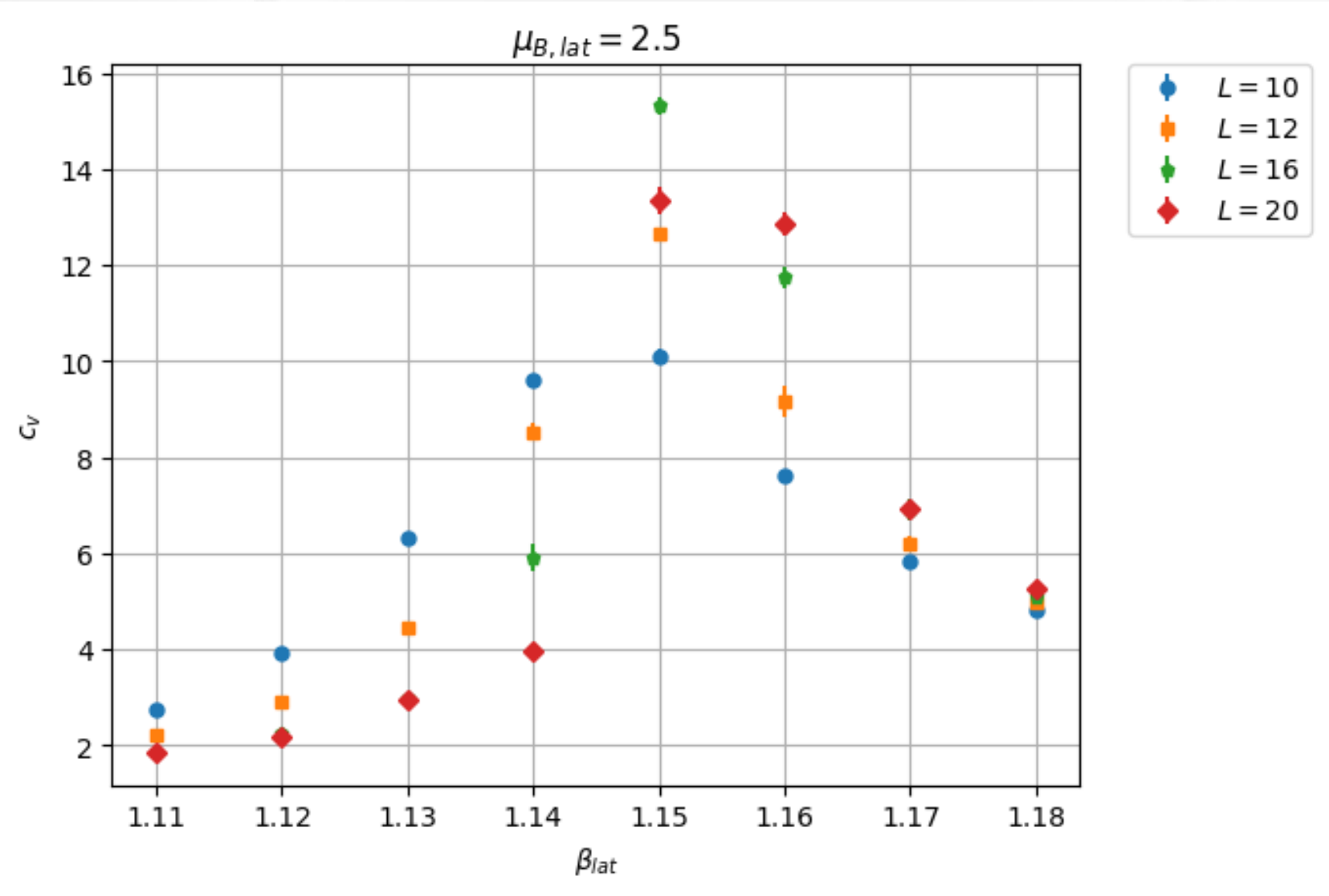

Specific heat at $\mu_{B,\mathrm{lat}} = 2.5$ in lattices of volume L^3.

Topological susceptibility

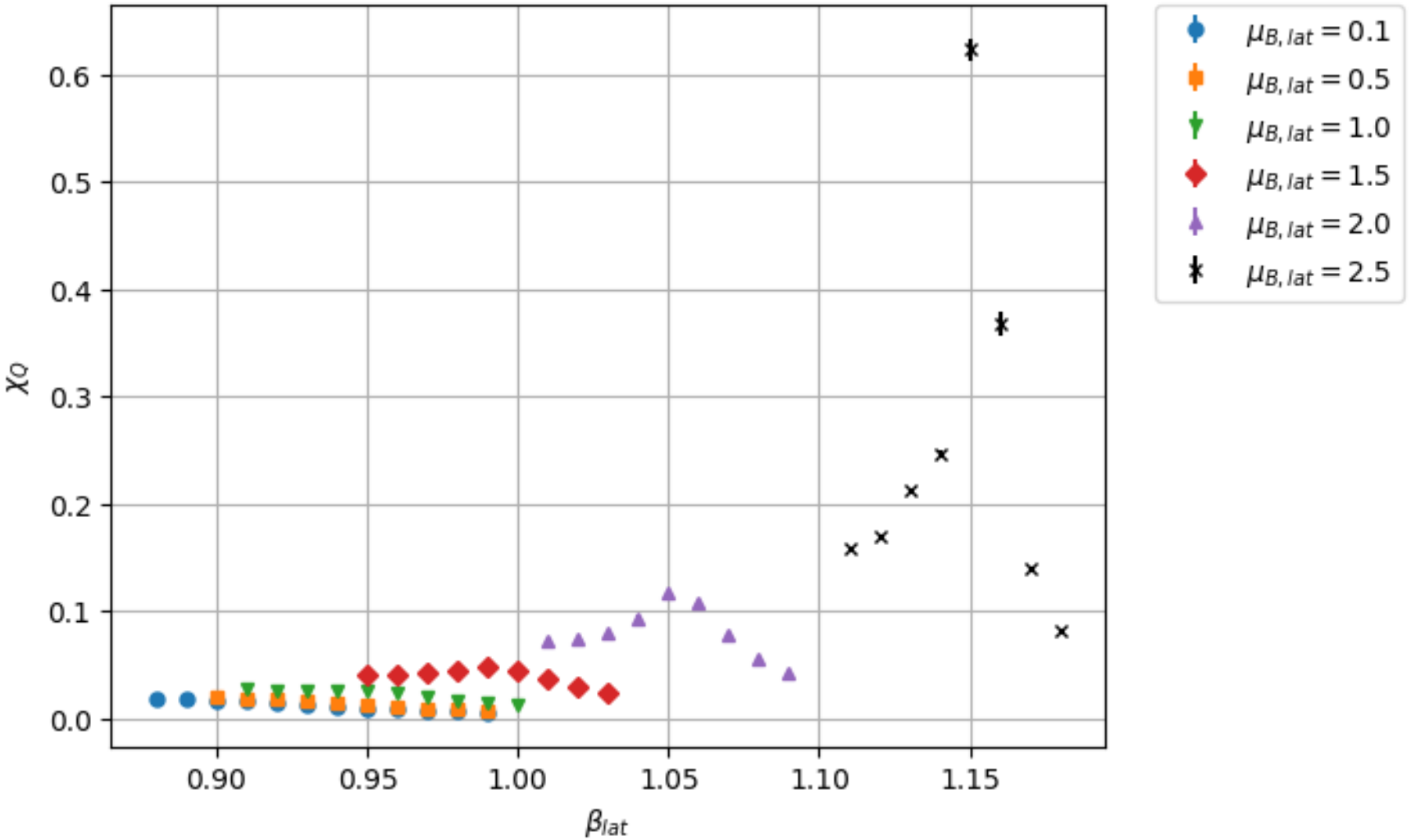

Topological susceptibility in a lattice of volume 20^3.

Critical exponents

- At $\mu_B = 0$, $\beta/\nu = 0.515$ and $\gamma/\nu = 1.970$ (Engels et al. 2003).
- Our results at $\mu_B = 0$, $\beta/\nu = 0.44(1)$ and $\gamma/\nu = 1.85(2)$.
- Finite-size effect.
- Errors are statistical, in addition large systematic errors due to the finite volume. At $\mu_B = 0$, consistent results but not precise.

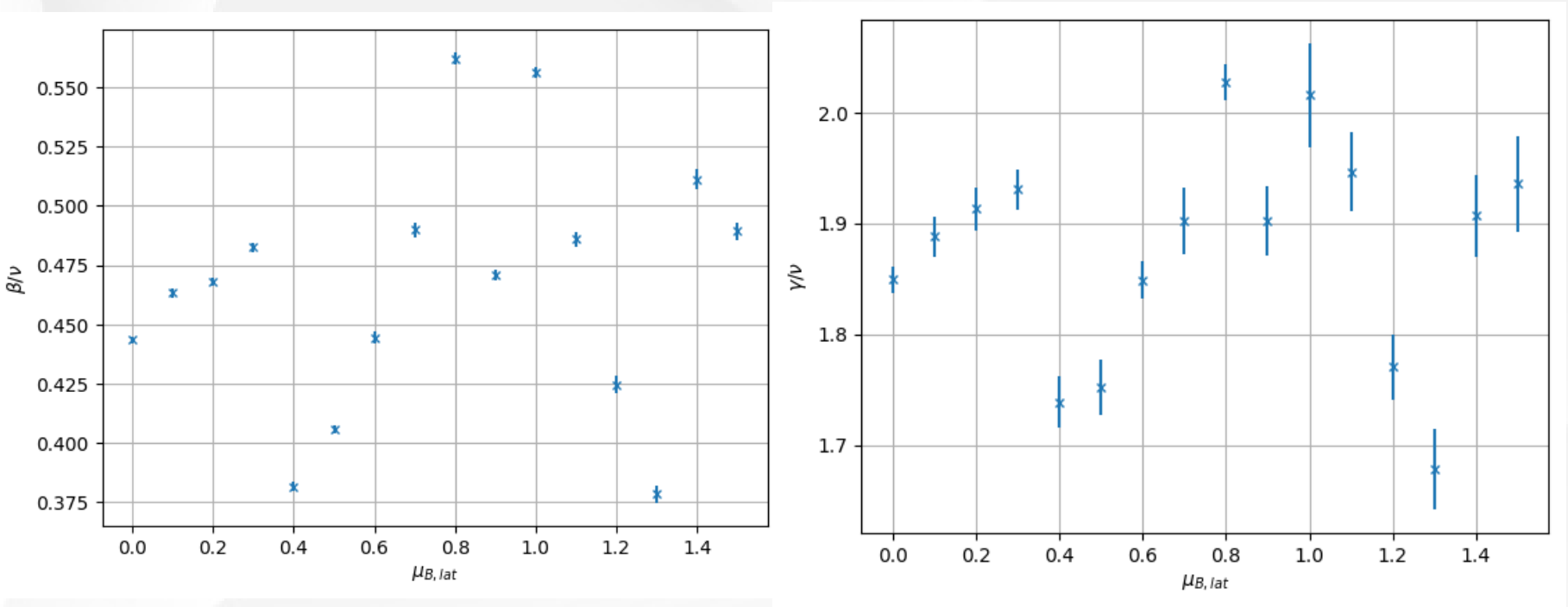

Left: Quotient of critical exponents β/ν as a function of temperature. **Right**: Quotient of critical exponents γ/ν as a function of μ_B.

Phase diagram

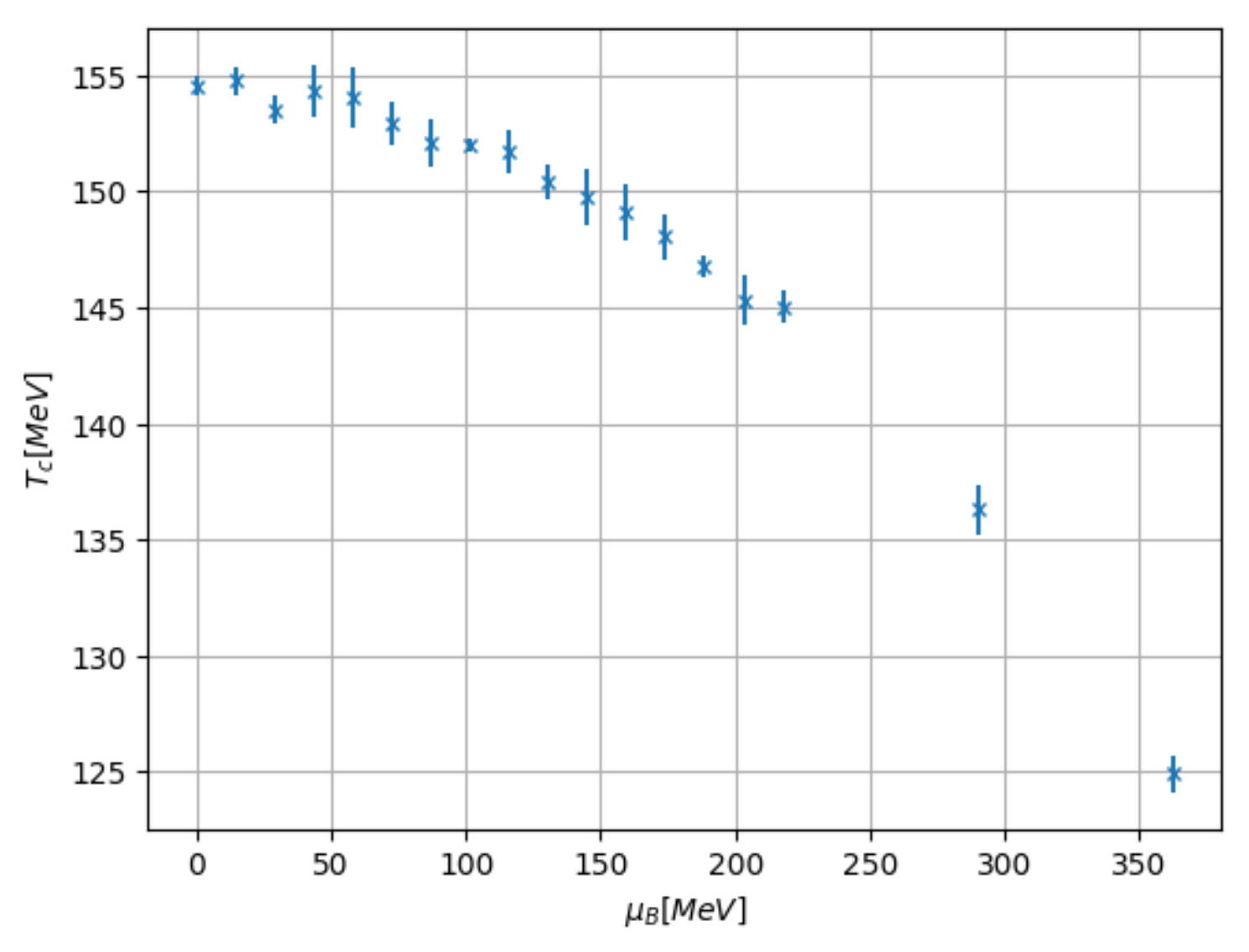

Phase diagram in physical units.

Phase diagram

Reference	$T_{\rm CEP}$[MeV]	$\mu_{B,{\rm CEP}}$[MeV]
Contrera et al. (2016)	69.9-128.6	223.3-319.1
Cui et al. (2017)	38	245
Kovácks and Wolf (2017)	53	885
Rougemont et al. (2017)	< 130	> 400
Sharma (2017)	< 145	$2T_{\rm CEP}$
Antoniou et. al (2018)	119-162	252-258
Ayala et al. (2018)	18-45	315-349
Goswami et al. (2018)	195.23-200.6	$\pi/3T_{\rm CEP}$
Knaute et al. (2018)	111.5	611.5
Li et al. (2019)	100	240
Martínez and Raya (2019)	49	310
Motta et al. (2019)	122	862
Zhao et al. (2019)	237	101
Ayala et al. (2020)	40-51	271-291
Wu et al. (2020)	69-72	813-971
Shi et al. (2020)	116-127	135-160
Zhao et al. (2020)	328-330	72-76
Our work	< 125	> 363

CEP estimations. For a previous table see Ayala et. al (2018).

Conclusion

- We have studied the 3d O(4) non-linear σ model, an effective theory of QCD with two flavors in the chiral limit.
- No solid evidence of μ_B-dependence of the critical exponents.
- The 3d O(4) model allow us to study the phase diagram of QCD with two flavors in the chiral limit at non-zero μ_B without sign problem.
- We could follow the critical line up to $\mu_B = 363$ MeV, where we find $T_c = 125$ MeV.
- The critical line is monotonically decreasing in μ_B.
- Only second order phase transitions up to $\mu_B = 363$ MeV.
- Possible indication of a first order phase transition at larger μ_B.

Bibliography

- G. S. Adkins, C. R. Nappi, and E. Witten. Nucl. Phys. B, 228:552–566, 1983.
- S. Borsanyi et al. (Wuppertal-Budapest Collaboration). JHEP, 09(073), 2010.
- J. Engels, L. Fromme, and M. Seniuch. Nucl.Phys. B, 675:533–554, 2003.
- J. Murakami. Proc. Amer. Math. Soc., 140(9):3289–3295, 2012.
- M. Oevers. Diploma thesis, Universität Bielefeld, 1996.
- T. H. R. Skyrme. Proc. Roy. Soc. A, 260:127–138, 1961; Nucl. Phys., 31:556–569, 1962.
- F. Wilczek. Int. J. Mod. Phys. A, 7(16):3911–3925, 1992.
- E. Witten. Nucl. Phys. B, 223:433–444, 1983.

Bibliography

- N. G. Antoniou, F. K. Diakonos, X. N. Maintas, and C. E. Tsagkarakis. Phys. Rev. D, 97:034015, 2018; A. Ayala, S. Hernández-Ortiz, and L. A. Hernández. Rev. Mex. Fís., 64:302–313, 2018; A. Ayala, S. Hernández-Ortiz, L. A. Hernández, V. Knapp-Pérez, andR. Zamora. Phys. Rev. D, 101:074023, 2020; G. A. Contrera, A. G. Grunfeld, and D. Blaschke. JHEP, 09(073), 2010; Z. F. Cui, J. L. Zhang, and H. S. Zong. Sci. Rep., 7:45937, 2017; J. Goswami, F. Karsch, A. Lahiri, M. Neumann, and C. Schmidt. PoS Proc. Sci., CORFU2018:162, 2018; J. Knaute, R. Yaresko, and B. Kämpfer. Phys. Lett. B, 778:419–425, 2018; P. Kovács and G. Wolf. Acta Phys. Pol. B Proc. Suppl., 10(4):1107–1112, 2017; B. L. Li, Z. F. Cui, B. W. Zhou, S. An, L. P. Zhang, and H. S. Zong. Nucl. Phys. B, 938:298–306, 2019; A. Martínez and A. Raya. arXiv:1909.12416 [hep-ph], 2019; M. Motta, M. Alberico, A. Beraudo, P. Costa, and R.. Stiele. arXiv:1909.05037 [hep-ph], 2019; R. Rougemont, R. Critelli, J. Noronha-Hostler, J. Noronha, and C. Ratti. Phys. Rev. D, 96:014032, 2017; S. Sharma. Nucl. Phys. A, 967:728–731, 2017; C. Shi, X. T. He, J. W. B., Q. W. Wang, S. S. Xu, and H. S. Zong. J. High Energ. Phys., 122:JHEP06, 2020; Z. Q. Wu, J. L. Ping, and H. S. Zong. arXiv:2009.13070 [nucl-th], 2020; Y. P. Zhao, R. R. Zhang, H. Zhang, and H. S. Zong. Chinese Phys. C, 43(6):063101, 2019.